

Article

Investigation of Mineral Oil and CuO Mixed Synthetic Oil in Compression Ignition Engines: A Comparison of Physicochemical Attributes

Aamir Sajjad Nasir ^{1,†}, Muhammad Usman ^{1,*}, Muhammad Ali Ijaz Malik ², Asad Naeem Shah ¹,
Ali Turab Jafry ³, Muhammad Wajid Saleem ⁴, Naseem Abbas ^{5,*}, Uzair Sajjad ⁶,
Mohammad Rezaul Karim ⁷ and Md Abul Kalam ²

¹ Mechanical Engineering Department, University of Engineering and Technology, G.T. Road, Lahore 54890, Pakistan; 2019msmet14@student.uet.edu.pk (A.S.N.); anaems@uet.edu.pk (A.N.S.)

² School of Civil and Environmental Engineering, FEIT, University of Technology Sydney, Sydney, NSW 2007, Australia; muhammadali.ijaz@superior.edu.pk (M.A.I.M.); mdabul.kalam@uts.edu.au (M.A.K.)

³ Faculty of Mechanical Engineering, Ghulam Ishaq Khan Institute of Engineering Sciences and Technology, Topi 23640, Pakistan; ali.turab@giki.edu.pk

⁴ Department of Mechanical and Energy Engineering, De Montfort University Dubai, Dubai 294345, United Arab Emirates; muhammad.saleem@dmu.ac.uk

⁵ Department of Mechanical Engineering, Sejong University, Gwangjin-gu, Seoul 05006, Republic of Korea

⁶ Department of Energy and Refrigerating Air-Conditioning Engineering, National Taipei University of Technology, Taipei 10608, Taiwan; uzairsajjad@mail.ntut.edu.tw

⁷ Department of Mechanical Engineering, College of Engineering, King Saud University, Riyadh 11421, Saudi Arabia; mkarim@ksu.edu.sa

* Correspondence: muhammadusman@uet.edu.pk (M.U.); naseem.abbas@sejong.ac.kr (N.A.)

† These authors contributed equally to this work.



Citation: Nasir, A.S.; Usman, M.; Malik, M.A.I.; Shah, A.N.; Jafry, A.T.; Saleem, M.W.; Abbas, N.; Sajjad, U.; Karim, M.R.; Kalam, M.A. Investigation of Mineral Oil and CuO Mixed Synthetic Oil in Compression Ignition Engines: A Comparison of Physicochemical Attributes. *Fire* **2023**, *6*, 467. <https://doi.org/10.3390/fire6120467>

Academic Editors: Mingjun Xu, Ruiyu Chen and Man Pun Wan

Received: 7 November 2023

Revised: 26 November 2023

Accepted: 27 November 2023

Published: 13 December 2023



Copyright: © 2023 by the authors. Licensee MDPI, Basel, Switzerland. This article is an open access article distributed under the terms and conditions of the Creative Commons Attribution (CC BY) license (<https://creativecommons.org/licenses/by/4.0/>).

Abstract: Mineral oil resources are depleting rapidly, and the slower conventional oil biodegradation process results in environmental pollution. To resolve this issue, cupric oxide (CuO) nanoparticles (1% wt) were introduced into a base oil to improve the lubricating capability of castor oil. In addition, 1% wt. sodium dodecyl sulfate was also blended with the base oil in order to attain the maximum dispersion stability of CuO nanoparticles in the castor oil. Afterward, thermophysical property, atomic absorption spectroscopy, and Fourier transform infrared radiation (FTIR) testing of the lubricant oil sample were performed before and after 100 h of engine operations at 75% throttle and 2200 rpm for each lubricant sample in order to check the capability of the novel oil with mineral oil. Compared with the natural mineral oil, the behavior of the CuO-based lubricant has essentially the same physical features, as measured according to ASTM standard methods. The physicochemical properties like $(KV)_{40\text{ }^{\circ}\text{C}}$, $(KV)_{100\text{ }^{\circ}\text{C}}$, FP, ash, and TBN decrease more in the case of the synthetic oil by 1.15, 1.11, 0.46, 1.1, and 1.2% than in the conventional oil, respectively. FTIR testing shows that the maximum peaks lie in the region of 500 to 1750 cm^{-1} , which shows the presence of C=O, C-N, and C-Br to a maximum extent in the lubricant oil sample. AAS testing shows that the synthetic oil has 21.64, 3.23, 21.44, and 1.23% higher chromium, iron, aluminum, and zinc content. However, the copper and calcium content in the synthetic oil is 14.72 and 17.68%, respectively. It can be concluded that novel bio-lubricants can be utilized as an alternative to those applications that are powered by naturally produced mineral oil after adding suitable additives that further enhance their performance.

Keywords: bio-lubricant; tribology; CuO-based nanoparticles; atomic absorption spectroscopy; lubricant oil degradation; Fourier transform infrared radiation

1. Introduction

Tribology is an emerging scientific area that deals with friction between mating surfaces and remedies to reduce friction and wear. The Organization for Economic Cooperation

and Development (OECD) first coined the term “Tribology” in 1967. Tribology deals with friction resulting from the interaction of mating surface and their remedies [1]. Both the wear scar diameter (WSD) and the coefficient of friction (COF) are analyzed profoundly in the field of tribology. Manufacturing companies usually suffer from significant financial losses due to lubrication failure and worn machine parts. The primary source of wear is friction, which results in energy loss. So, to deal with friction, it is evident that enormous resources have been imported for use [2]. It is estimated that 28% of the total energy extracted from petroleum fuels is squandered as a frictional force inside the engine and vehicle propulsion [3]. Depending on vehicle speed, around 10% of fuel energy is consumed in overcoming aerodynamic drag, and such frictional losses ultimately result in higher fuel consumption. Moreover, an in-depth analysis of passenger vehicles revealed that around 60% of the total fuel energy dissipates as frictional losses in the combustion chamber [4].

The tribological advancements in the USA are solely responsible for an annual saving of around 11% in energy in the power sector, industrial sector, turbo-machinery sector, and transportation sector [5]. It is further stated that the tribological advancements have the potential to save almost 18.6% of the total annual energy, equivalent to USD 14.3 billion per annum [6]. Lubricant oil served as the prime factor in the smooth operations of internal combustion (IC) engines. Conventional lube oils have been in use for decades to reduce wear and friction. There are two main issues associated with crude oils, one is a hike in their prices and the second is their non-biodegradability, as they are dumped into the environment and result in pollution. However, mineral oils can be regenerated [7,8] or their properties can be enhanced with the use of additives [9,10] so that energy conservation can take place. Different lubricants including semi-solids (grease) and liquids (oils) are available on the market, but liquid lubricants in the automotive industry are the most widely accessible. When a lubricant overcomes tribological issues at high temperatures, it is regarded as effective [11]. The environmental consequences and economic viability are also considered throughout the selection process of a lubricant [12]. Mineral carbonation technology is currently emerging in order to reduce the greenhouse gases [13]. The critical lubricant characteristics in automotive engines proposed by previous researchers are the viscosity (dynamic and kinematic), pour point (PP), shear stability, volatility, cloud point (CP), foaming attributes, metallic particles, flash point (FP), density, ash content, moisture content, rust color, corrosion resistance, elastomer compatibility, and homogeneity [14]. In many ways, conventional mineral oils affect and degrade ecosystems as CO₂ emissions cause global warming and residual mineral oil disposal pollutes soil and water.

It is important to mention that vegetable oils are biodegradable to an extent of 70 to 100% due to microorganisms. Mineral oils, on the other hand, have a biodegradability of 15 to 35% [15,16]. The biodegradability of vegetable oils can further be modified and improved in order to use bio-lubricants as an alternate source to mineral oils. Esterification/transesterification, selective hydrogenation, Estolide production, epoxidation, and introducing additives into the base oil are some of the approaches used to modify lubricant oil characteristics [17]. The primary purpose of lubricants with additives is to improve the tribological properties of the surfaces in contact, which ultimately reflects in engine performance and durability improvement. Surface additives are important in tribology for reducing friction and rebuilding worn surfaces among mating surfaces [18]. High-load contacts include the piston skirt cylinder liner, piston ring liner, and cam follower, which run under mixed and boundary lubrication regimes. Friction modifiers are utilized to minimize friction in these areas [19]. Furthermore, it was also reported that rapeseed and Karana oils are utilized to enhance the engine performance features by providing good lubrication. On the other hand, engine emissions can be minimized by utilizing castor oil and palm oil [20]. For the oil–fuel ratio of 1%, a lubricating oil made from castor oil will minimize smokey emissions by 50 to 70%. Thus, castor oil can serve as a smoke pollution reducer [21].

The tribological characteristics of base castor oil and high-quality crankcase oil (20W-50) were compared using four-ball testing. Castor oil served as an excellent choice for

crankcase oil and plant engines because it not only provides ecological and tribological advantages but also provides food security [22]. It was also reported that CuO with palm oil at concentrations of 0.25, 0.5, 0.75, 1, 1.25, and 1.5% increased the anti-wear and high-pressure characteristics [23]. Another study was conducted for the development of castor oil-based lubricant. MoS₂ and CuO particles with a size of 50 nm diameter were suspended in the castor oil at various concentrations. The coefficient of friction was measured using a QG700 tribometer with Si₃N₄ ball material. With an increase in the concentration of 0.1 wt% of MoS₂ and CuO particles, a decrease in the coefficient of friction of 17.6% and 20% was observed at a load of 25 N and a speed of 2370 rpm [24].

The tribological characteristics of steel alloy (CK50) and aluminum alloy (2024-T4) were investigated using various proportions of CuO and MoS₂ in molding and castor oil. A pin-on-disk test was performed to determine the coefficient of friction (COF) and wear rate, sodium dodecyl sulfate was used as a dispersant in the base oil to prevent nanoparticle suspension difficulties. The COF was decreased by making use of MoS₂ (1% by wt.) in the castor oil [25]. Imran et al. [26] used different nanoparticles in biodiesel blends (CuO, TiO₂, CNT, Al₂O₃, GNP, and CeO₂) to compare their impact on engine performance and emissions. They found the most promising results for CuO-blended fuel in terms of both emissions and engine performance.

Rehim and Elsoudy [27] observed a decrease of 37.9, 42.9, and 14.6% in the COF for CuO nanoparticle concentrations of 0.2, 0.5, and 1% wt., respectively. A lower zeta potential value signifies a feeble electrostatic repulsive stabilization among the CuO nanoparticles enveloped by oleic acid (OA). As a surfactant, OA assumes the role of steric stabilization by coating CuO nanoparticles, thereby transforming their hydrophilic nature into a hydrophobic state and subsequently mitigating aggregation. CuO nanoparticles demonstrated commendable tribological performance when incorporated into HD 50 Engine Oil (SAE 50) as an additive, with concentrations ranging between 0.25 and 1.45 wt%. The tribological tests, which were conducted using a pin-on-disc tribotester, revealed that the COF reached its minimum value when the concentration of CuO nanoparticles was 1 wt%. Beyond this optimal concentration, the aggregation of nanoparticles led to an elevated COF. At the optimal nanoparticle concentration, the COF exhibited a substantial reduction of 53.98% compared with engine oil devoid of nanoparticle additives [28]. The introduction of CuO nanoparticles demonstrated a synergistic relationship with PAO, leading to a diminished COF in contrast with PAO without the nanoparticle additive. Utilizing 0.5 wt% of CuO nanoparticles in PAO yielded a considerable 6.96% reduction in the COF compared with PAO without the inclusion of nanoparticles [29]. Moreover, the utilization of CuO nanoparticles in SAE 20W-50 led to a reduction in the COF when compared with the oil without nanoparticle additives. Tribological experiments using a pin-on-disk configuration were executed, incorporating nanoparticles at concentrations spanning from 0.25 to 1 wt%. The findings revealed around an 11.14% decrease in the COF relative to nanoparticle-free oil when 0.25 wt% of CuO nanoparticles were used [30].

Popala et al. [31] used varying proportions of CuO nanoparticles (0, 0.75, and 1.50 wt%) in lubricant oil and assessed their tribological characteristics using a ball-on-disc tribometer. Different loadings (2, 5, and 8 N) along with variable speed conditions (150, 200, and 250 rpm) were used in their analysis. The output parameters included flash temperature, COF, and wear rate. It was observed that the lowest COF of 0.048, minimum wear rate of 0.012, and highest flash temperature of 0.035 were at speeds of 250 rpm, 200 rpm, and 250 rpm, respectively, while the concentration and load were 0.75% and 5 N. Moreover, the optimized conditions to minimize the wear rate and COF and maximize the flash temperatures were identified at a concentration of 1.1061 wt%, a speed of 217.6768 rpm, and a load of 5.0909 N. Baskar et al. [32] investigated the tribological performance of journal bearings using SAE20W40 synthetic lubricant and chemically modified rapeseed oil (CMRO) as a bio lubricant, both dispersed with CuO, WS₂, and TiO₂ nanoparticles as anti-wear additives. The journal-bearing test rig was used to assess the COF, wear rates, and oil film thickness at a load of 10 kN l and a speed of 3000 rpm. The most favorable outcomes

were observed with lubricant oil containing CuO as additives, showcasing a 27% reduction in the COF and a 47% decrease in the wear rate compared with synthetic lubricant.

Different mixing methods for CuO dispersion in base oil are used, but ultrasonication is the most widely used technique to achieve a higher dispersion rate. Sukkar et al. [33] used bath ultrasonication and mechanical mixing techniques to disperse nanoparticles (CuO and TiO₂). These techniques were used to achieve higher dispersion rates with the operating conditions of power (100%), temperature (40 °C), time (2–3 h), and frequency (20 kHz). Fayad et al. [34] used an electric magnetic stirrer continuously for 30 min to prepare a mixture. To reach equilibrium at room temperature, the nanoparticles (NPs) and base oil were left for 30 min before they were subjected to any test. Esfe et al. [35] used a magnetic agitator for mixing, suspension, and initial dispersion of a hybrid nanofluid. Ultrasound was also used for 1 h to remove sediment and prevent the formation of cluster nanoparticles. Sonication is a physical method that uses ultrasound to fluid and can be used to increase the stability of hybrid nanofluids by breaking the gravitational force of nanoparticles in sediments. Tabbakh et al. [36] used a mechanical stirrer to mix 0.1, 0.5, 1, and 1.5 g of copper oxide material with 100 mL of 60 stock (base oil), maintaining weight in the presence of 10 g of oleic acid for 10 min before blending with the base oil.

The environmental impact, coupled with concerns about resource depletion, underscores the necessity for a paradigm shift towards sustainable alternatives from conventional lubricants. The existing literature highlights the ecological drawbacks of conventional lubricants, underscoring a critical need for bio-based solutions. Bio-lubricants, typically derived from renewable resources such as vegetable oils or animal fats, offer a promising avenue for mitigating these environmental concerns. However, despite the potential advantages, there exists a notable gap in the literature regarding the widespread adoption and performance optimization of bio-lubricants in the automotive sector. The current research seeks to address this gap by systematically exploring the synthesis, characterization, and application of bio-lubricants as viable replacements for conventional lubricants. By conducting a comprehensive study, the current study aims to provide a deeper understanding of the overall performance of bio-lubricants in comparison with their traditional counterparts. The combination of castor oil, CuO nanoparticles, and sodium dodecyl sulfate as a dispersant has never been used before for the synthesis of bio-lubricants. The objective of current research is to substitute synthetic lubricants with conventional lubricants due to their biodegradable nature, better economy, and lower hazardous emissions. From Table 1, it is clear that no such comprehensive study has been conducted so far to evaluate the performance of cupric oxide synthetic oil including three types of testing (physicochemical testing, infrared testing, and spectroscopy testing), collectively.

Table 1. Comparison between the current study and previous studies.

Reference	Lubricant Oil Synthesis Composition	Lubricant Oil Testing		
		Physicochemical Testing	FTIR Testing	AAS Testing
Navada et al. [37]	CuO + pongamia oil	✓	✓	✗
Kumar et al. [38]	CuO + sunflower oil	✗	✓	✗
Gupta et al. [39]	CuO + 5W30 engine oil	✓	✓	✗
Subedi et al. [40]	CuO + 20W50 engine oil	✓	✓	✗
Ghaednia et al. [41]	CuO + sodium oleate	✓	✗	✗
Shah et al. [42]	CuO + hybrid paraffin oil	✗	✗	✗
Tabbakh et al. [36]	CuO + 60 stock (base oil)	✓	✓	✗
Current study	CuO + castor oil	✓	✓	✓

2. Materials and Methods

Figure 1 displays the activity work plan for this experimental study. Moreover, the following subsections comprehensively explain every step involved in the methodology section.

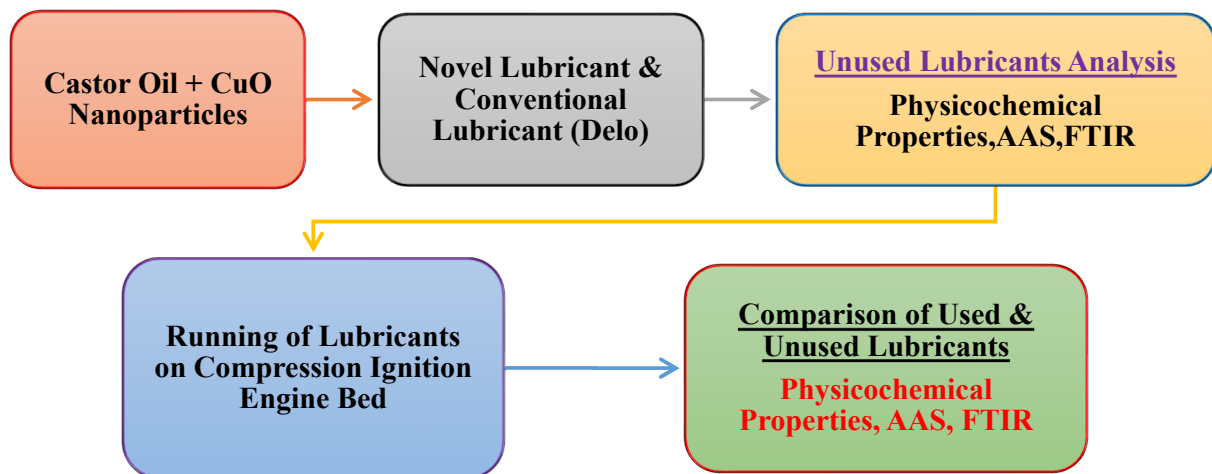


Figure 1. Methodology flowchart.

2.1. Lubricant Oil Synthesis

Different materials were utilized to examine the tribological impact of the synthetic lubricant oils. The specifications and properties are discussed below:

2.1.1. Base Oil

A commercially available base oil was utilized to make the synthetic lubricant with different bio-lubricants (edible and non-edible). Castor oil was chosen as the base oil in the preparation of synthetic lubricants due to its lower iodine value (83.5 gI₂/100 g) and acid number (0.91 mgKOH/g) along with higher density (962.8 kg/m³), saponification (179.4 mgKOH/g), specific gravity (0.959), and pH value (7.2) [43]. Table 2 depicts the characteristics of castor oil:

Table 2. Castor oil physicochemical properties.

Properties	Units	Castor Oil
Cloud point	°C	14.6
Density	kg/m ³	957.9
Pour point	°C	−25
Fire point	°C	340
Viscosity	mpa.s	684.36
Flash point	°C	290
Specific gravity	-	0.9737
Calorific value	MJ/kg	38.34
Cetane rating	-	43.7
Oxidation stability	H	4.4

2.1.2. CuO Nanoadditives

The nanoparticle (NP) additive used in the current study was cupric oxide (CuO). The CuO nanoparticle was purchased from the company Sigma Aldrich (St. Louis, MO, USA), which had a 60 nm average particle size and a black appearance. CuO as an additive was chosen to improve the lubrication's performance by reducing the lubricant's wear-and-tear in the engine. Additionally, these additives reduce exhaust emissions. In the presence of carbon atoms, CuO behaves like a catalyst and decreases the oxidation temperature. Furthermore, it accelerates the oxidation of soot particles by developing more hydroxyl radicals from the water molecules [44]. The higher surface-to-volume ratio of the particles results in the better oxidation of hydrocarbons. NPs act as oxygen buffers and result in higher air–fuel mixing rates and fuel combustion. NP additives in diesel/biodiesel fuel reduce their evaporation time and result in a lower ignition delay (ID). These NP attributes result in higher brake thermal efficiency (BTE) and heat release rate (HRR) during the

combustion process [45]. CuO also aids in boosting the FP temperature as well as the cetane rating of biodiesel by acting as a combustion catalyst for hydrocarbon fuels [46]. However, the uniform dispersion of NPs is mandatory in order to accomplish improved combustion. Table 3 depicts the properties of CuO nanoparticles.

Table 3. CuO NPs specifications.

Suppliers Information	CuO
Company	Sigma Aldrich (St. Louis, MO, USA)
Grade standard	Electron grade
Purity	99%
Average particle size (nm)	60
Appearance	Black powder

2.1.3. Dispersant

It was observed that the nanoparticles settled in the bottle after 72 h when these nanoparticles were added to the castor oil utilizing a hot plate and sonication bath. The reason for their settling was the formation of amalgamation because of Van Der Waal forces between the particles. A sodium dodecyl sulfate with a concentration of 1.5% was utilized as a dispersant in order to ensure dispersion stability and to overcome the sedimentation issue of CuO nanoparticles in castor oil. Sodium dodecyl sulfate served as a primary constituent in keeping nanoparticles dispersed in the castor oil.

2.2. Engine Specifications

Experiments were carried out on a C.I. engine of UET Lahore's Automobile Department. A diesel engine (Lombardini-15 LD 315) was operated at 2200 rpm under 75% open throttle (OT) for 100 h of operational running. The novel lubricant based on CuO and the mineral lubricant (Delo) were poured into an oil sump tank, which operated for about 100 h of each separately. The technical specifications of the diesel engine are displayed in Table 4.

Table 4. Compression-ignition engine specifications.

Description	Specifications
Cylinders	1
Bore	78 mm
Displacement	315 cm ³
Stroke	60 mm
Oil consumption	0.0030 L
Oil sump capacity	1.2 L
Dynamometer attached	Hydraulic dynamometer
Cooling System	Air-cooled
Mode of injection	Direct Injection
Compression ratio	20.3:1
Dry weight	33 kg
Max. torque @ rpm	15 Nm @ 2400
Recommended battery	12/44 (V/Ah)

2.3. Blend Making

In the lab of the Chemical Engineering Department at UET, Lahore, a 1500 mL beaker, a digital weight balance, a hot plate, and a sonication bath were utilized to make a blend of 1.2 L, as the oil sump capacity of the diesel engine was 1.2 L. First, 1.2 L of castor oil was poured into the beaker according to the requirement and placed on the hot plate with a magnetic stirrer in it. After that, copper oxide (CuO) nanoparticles (0.1 g) and dispersant sodium dodecyl sulfate (1 g) were weighted using a digital weight balance available in the lab. Then, weighted concentrations of nanoparticles and dispersant were blended into the castor oil. The temperature of the hot plate was set at 40 °C. For proper dispersion of

nanoparticles in the oil, the lubricant oil sample was stirred for about 45 min. Furthermore, the blend was placed in a sonication bath for about 45 min at 40 °C for more dispersion stability of the nanoparticles in the oil. Our literature review suggested that 40 to 60 min is enough for the proper dispersion of nanoparticles in lubricant oil [47,48]. After proper consideration and taking into account the experimental conditions, the 45 min stirring time was selected in order to avoid agglomeration. Finally, the blend was stored in a glass bottle to observe the dispersion stability of the additive.

2.4. Lubricant Testing

After 72 h, sodium dodecyl sulfate was added to the novel castor-based oil blend to resolve the problem of dispersion of nanoparticles in the oil. The fresh synthetic lubricant was then ready for testing. To examine the physicochemical properties of the lubricant, 500 mL of a sample was also prepared in the lab. The sample was then distributed to various departmental labs including Chemical, Polymer, Petroleum, and Environmental Engineering of UET Lahore for the examination of the kinematic viscosity (KV) at 100 and 40 °C, ash content, flash point (FP), pour point (PP), total base number (TBN), and specific gravity (SG). The physicochemical properties of the conventional lubricant oil were taken from Caltex Pakistan Ltd. Furthermore, the AAS Machine of Agilent Technologies 200 Series AA (Agilent Technologies, Santa Clara, CA, USA) was utilized for metallic elements detection including iron (Fe), zinc (Zn), copper (Cu), aluminum (Al), chromium (Cr), and calcium (Ca) in both the novel and conventional lubricants. Finally, an FTIR analysis of both novel and conventional lubricants was performed. In the Department of Humanitarian Sciences at the UET, Lahore, both AAS and FTIR analysis were performed as presented in Figure 2a,b, respectively.

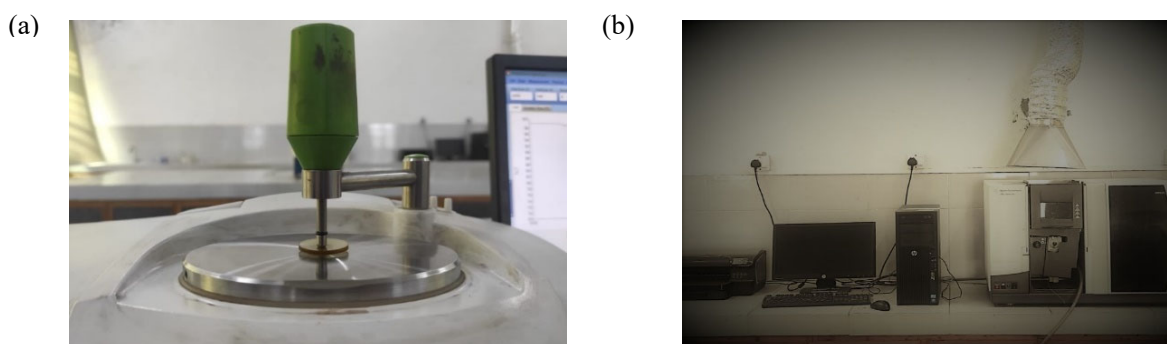


Figure 2. (a) FTIR of a lubricant sample. (b) AAS of the sample lubricants for element detection.

2.4.1. Fresh Novel and Conventional Lubricant Testing

When the examination and analysis of the CuO-based novel lubricant and mineral lubricant (Delo) were complete, the novel lubricant was put into an oil sump and the engine was operated at 2200 rpm for 100 h. Furthermore, the conventional oil (Delo) was also run on a C.I. engine for another 100 h.

2.4.2. Testing of the Used CuO-Based Novel and Delo-Based Conventional Lubricants

To study the tribological alterations and determine the structural changes in the lubricants, a physicochemical properties analysis, AAS, and FTIR were performed on the used samples.

2.4.3. Comparison

To examine the tribological behavior and tribological changes in the CuO-based novel and mineral (Delo) lubricants, the variation in physicochemical properties, AAS, and FTIR were compared for conclusions. Table 5 entails all the constituents of the experimental study.

Table 5. Experimental study constituents.

Parameters	Description
Lubricant oil	Mineral oil and synthetic oil
Deterioration time	A total of 100 h of engine operations
Physicochemical testing	Kinematic viscosity at 100 and 40 °C, ash content, flash point, pour point, total base number, and specific gravity
FTIR testing	O-H, C-H, C=O, C-N and C-Br functional group
AAS testing	Iron, copper, chromium, zinc, calcium and aluminum

3. Results

The physicochemical properties analysis, infrared, and atomic absorption spectroscopy results depict the performance of the synthetic oil in comparison with the mineral oil.

3.1. Physicochemical Property Analysis

To determine the compatibility of the novel lubricant as an alternative to the mineral lubricant (Delo), the physicochemical properties of both lubricants were compared. The mineral lubricant Delo Gold Ultra SAE 15W-40, API CI-4/SL multigrade oil was selected as the standard for the examination, as per the recommendations of the engine manufacturer. Table 6 displays the properties of the mineral oil (MO). The variation in physicochemical properties for both the mineral and synthetic oils (SO) are explained below:

Table 6. Mineral oil (Delo 15W40) specifications.

Mineral Oil (MO)	Measuring Units	Test Standards	Properties
TBN	mg KOH/g	D2896 [49]	10.2
(KV) _{40°C}	mm ² /s	D445 [50]	115
(KV) _{100°C}	mm ² /s	D445 [50]	15.1
Sulfated ash	% by mass	D784 [51]	1.4
Viscosity index	-	D2270 [52]	137

3.1.1. Kinematic Viscosity

At the same temperature, the kinematic viscosity is the relative ratio of fluid dynamic viscosity to density. The kinematic viscosity (KV) of lubricant oil usually decreases with a temperature increase, as shown in Figure 3. The ASTM D445 standard [50] was used in order to determine the KV. For proper lubricant oil functioning, the KV should be optimum as a high KV results in using engine power to pump lubricant oil into engine cooling channels, which ultimately causes brake power to decrease. If KV is too high, lower lubricant oil layers will be unable to cover the space between intersecting surfaces, which results in high friction [53]. The molecular breakdown and fuel dilution in lubricant oil are the main reasons for the decline in kinematic viscosities [54].

The (KV)_{40 °C} of the mineral lubricant (Delo) reduced from 115 mm²/s to 99.3 mm²/s, with a depreciation of 13.65%. However, the KV of the CuO-based novel lubricant was reduced from 240 mm²/s to 210 mm²/s, with a depreciation of 12.5%. The mineral lubricant deteriorated 1.15% more than the CuO-based novel lubricant at 40 °C. The kinematic viscosity of the mineral lubricant decreased from 15.1 mm²/s to 13.2 mm²/s at 100 °C. The mineral oil deteriorated by 12.58%. On the contrary, the KV of the CuO-based novel lubricant declined from 17 mm²/s to 15.05 mm²/s. The mineral lubricant deteriorated 1.11% more than the CuO-based novel lubricant at 100 °C. The decrease in kinematic viscosity of oil can be credited to the dilution of fuel and molecular breakdown of lubricant with an increase in temperature [55].

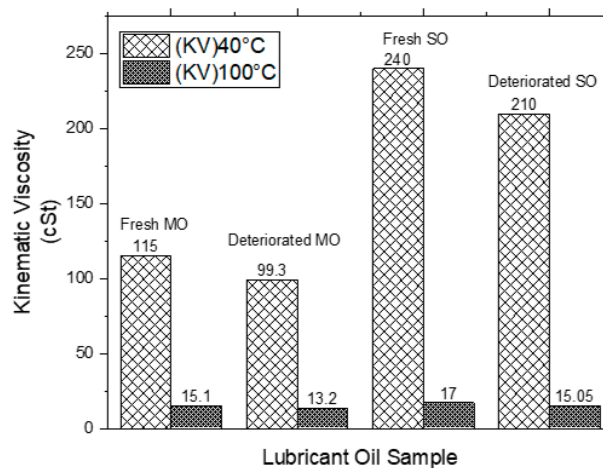


Figure 3. Comparison of $(KV)_{40^{\circ}\text{C}}$ and $(KV)_{100^{\circ}\text{C}}$ before and after the use of the samples.

3.1.2. Pour Point (PP)

Under standard cooling parameters, the minimum lubricant oil temperature at which it can be poured or flow under the action of gravity is known as the pour point. A PP is the temperature at which fuel loses its flowability and becomes too viscous to pour. In other words, it is a measure of the fuel's ability to flow at low temperatures. A higher pour point means that the fuel will become more viscous and difficult to flow at lower temperatures. This can result in fuel line blockages and insufficient fuel supply to the engine, leading to starting difficulties and poor engine performance in cold weather. Therefore, a lower pour point is desired to ensure proper fuel flow and prevent operational issues during cold starts. Figure 4 shows a decrease in the PP with the increase in temperature.

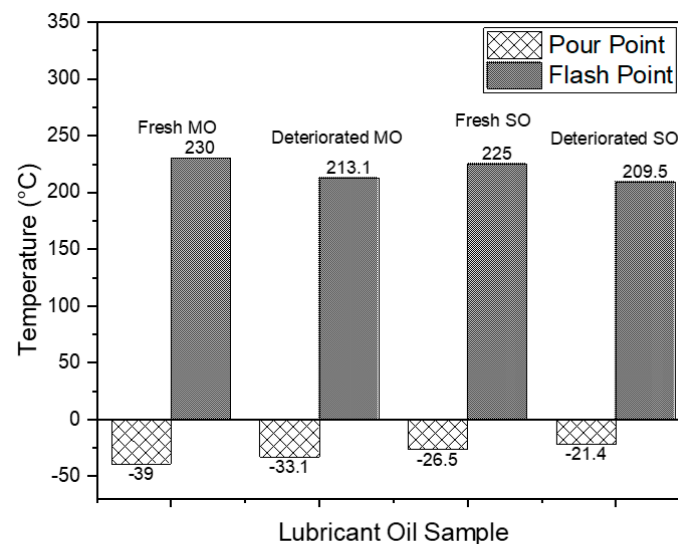


Figure 4. Comparison of the pour point and the flash point before and after using the samples.

The PP of the mineral lubricant declined from -39°C to -33.1°C and resulted in a deterioration of 15.1%. During engine operations, the temperature of lubricant oil may increase due to the heat generated by the engine. This increase in temperature generally leads to a decrease in the viscosity of lubricant oil, making it flow better. However, the change in temperature primarily affects the pour point of the lubricant oil, as observed in the decline in the pour point after running the engine for 100 h. On the contrary, the pour point of the CuO-based novel lubricant decreased from -26.5°C to -21.4°C and resulted in a higher deterioration of oil, i.e., 19.24%. The mineral oil gives better results as compared with the CuO-based novel oil as far as the pour point is concerned.

3.1.3. Flash Point (FP)

The minimum temperature of the lubricant at which it produces an ignitable vapor blend is known as the flash point. In diesel engines, the value of the flash point decreases as the temperature increases. The ASTM D92 standard [56] was followed by determining the FP of the conventional and synthetic lubricant oils. The FP indicates the fire safety of lubricant oil applications as it is used to define its maximum functional limit. The malfunctioning of lubricant oil may take place in the case of a lower FP [57]. Figure 4 shows the declining trend in the FP in the case of the mineral lubricant (Delo-Gold Ultra SAE 15W-40 multifunctional C.I. engine oil) from 230 °C to 213.1 °C. The mineral oil deteriorated by 7.34% with the increase in temperature. On the contrary, the CuO-based novel lubricant flash point decreased from 225 °C to 209.5 °C and resulted in a deterioration of 6.88% with an increase in temperature. The decrease in flash points of both lubricants was in the acceptable range.

3.1.4. Total Base Number

The property of the lubricants that reflects the capability to control the acidity generated during the combustion process inside engine cylinder is known as the total base number. This property indicates how much acidity will be produced in the engine and how long the lubricants will last.

A lubricant oil serviceability depends on total base number (TBN) as it indicates alkaline derivatives in lubricant oil. A lower TBN indicates higher corrosion and poor performance. On the contrary, a higher TBN indicates higher antioxidation capacity [58]. A TBN with an alkaline nature is desirable for effective engine performance and corrosion deterrence [50]. The ASTM D-2896 standard [49] was used to determine the TBN value of the lubricant oil. Figure 5 shows the decline in the TBN during diesel engine operations due to higher acidic traces of combustion in the oil. The TBN of the mineral lubricant decreased from 10.2 mg KOH/g to 8.5 mg KOH/g. The TBN of the mineral lubricant deteriorated by about 16.66% during the operation of the C.I. engine. On the contrary, the TBN of the CuO-based novel lubricant decreased from 8.6 mg KOH/g to 7.3 mg KOH/g, and the novel lubricant oil deteriorated by 15.11%. The deterioration difference between the CuO-based lubricant and the convention lubricant is comparable. The performance of the CuO-based novel lubricant is similar to the mineral lubricant in terms of changes in TBN.

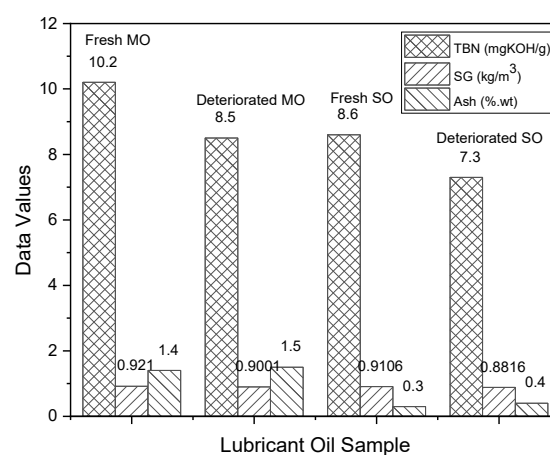


Figure 5. Comparison of TBN, specific gravity, and ash in the lubricant oil samples before and after use.

3.1.5. Specific Gravity

At a specified temperature and pressure, the specific gravity (SG) is the ratio of the tested fluid density to water. It is a dimensionless quantity and has no units because it is a ratio between two similar properties. Specific gravity is directly linked with load-bearing

capabilities. A lubricant oil with a higher specific gravity can bear more load as compared with a lubricant oil with a lower specific gravity [59]. As the temperature in the C.I. engine increases, the specific gravity value decreases (see Figure 5). The specific gravity of the mineral lubricant oil decreased from 0.9210 kg/m^3 to 0.9001 kg/m^3 with a depreciation of 2.26%, while the specific gravity of the CuO-based novel lubricant decreased from 0.9106 kg/m^3 to 0.8816 kg/m^3 with a depreciation of 3.18%. The deterioration difference is merely 1.06%.

3.1.6. Ash Content

The measure of the number of residual materials that are not volatile when ignited in the vicinity of sulfuric acid (H_2SO_4) is known as sulfated ash examination. A lubricant oil's purity can be evaluated using its ash content. Ash content depicts the proportion of solid waste present in lubricant oil after the combustion cycle [60]. Moreover, it denotes non-combustible constituents (atmospheric dust, thermally decomposed particles, wear debris, and sludges) that exist as ash during the post-fuel combustion phase [61]. Engine lube oil additives, gasoline, engine wear, and rust in engines are the main sources of ash. In a used lubricant, the ash content increases, as depicted in Figure 5. The ash content of the mineral lubricant increased from 1.4 m% to 1.5 m% after 100 h of engine operation. While on the contrary, the ash content of the novel lubricant increased from 0.3 m% to 0.4 m%. It is obvious from the results that the novel lubricant performs much better than the mineral lubricant regarding ash content.

3.2. Fourier Transform Infrared (FTIR) Spectroscopy

FTIR analysis is a technique for identifying organic, inorganic, and polymeric elements in samples by scanning them with infrared light [62,63]. To determine the presence of distinct functional groups in a specimen, Fourier transform infrared spectroscopy (FTIR) is utilized. Figure 6 illustrates the chemical characterization of the four lubricant oil samples based on variation in the FTIR spectra. Figure 6 shows a comparison between the behavior of the mineral and synthetic oils for both the deteriorated and fresh samples. In Fourier transform infrared (FTIR) spectroscopy, transmittance is a measure of the amount of infrared light that passes through a sample at different wavelengths. Transmittance is often expressed as a percentage, where 100% transmittance means that all the infrared light passes through the sample, and 0% transmittance means that none of the light passes through (all absorbed by the sample). The lower transmittance in an FTIR spectrum indicates that more infrared light has been absorbed by the sample. Absorption of infrared light corresponds to the presence of specific functional groups or chemical bonds in the sample. The absorption pattern in the lower transmittance region provides diagnostic information about the chemical structure of the sample.

Figure 6 shows distinct regions of the synthetic lubricant (fresh and deteriorated) and conventional lubricant (fresh and deteriorated). Different peaks at distinct wavenumbers show the presence of a specific functional group [64–66]. In the case of synthetic lubricants, a first narrow peak starts at nearly the $3187\text{--}3628 \text{ cm}^{-1}$ wavenumbers. The hydroxyl (O-H) functional group is associated with the first peak for synthetic lubricants when compared with the IR chart. The presence of the hydroxyl group in synthetic oil depicts enhanced biodegradability, and the protective layers on metal surfaces help to prevent corrosion and wear. However, the hydroxyl group makes synthetic oil more susceptible to hydrolysis and oxidation, especially in the presence of water or moisture. It results in the breakdown of additives and base oil molecules, impacting the lubricant's overall stability and performance.

A second narrow stretch peak shows the presence of the alkane (C-H) functional group. A third peak around 2926 cm^{-1} in the single-bonded region shows that it has another alkane group. The subsequent two peaks were formed at 2882 and 2856 cm^{-1} , depicting the presence of an alkane functional group. Fresh lubricant oils, including both mineral and synthetic oils, depicted higher peaks than deteriorated oils, which showed the

presence of an alkane group in fresh lubricant oils. The saturated alkanes contribute to the overall viscosity of the lubricant. The length and branching of alkane chains influence the viscosity characteristics of the oil. Longer and less branched alkane chains generally result in higher viscosity. Alkane groups provide a slippery film that helps to reduce friction between moving parts. The lubricity of a lubricant, or its ability to reduce friction and wear, is influenced by the nature and arrangement of alkane chains. Saturated alkanes contribute to the thermal or oxidative stability of the lubricant. They can resist thermal breakdown and maintain their lubricating properties at high temperatures, which is crucial in applications where lubricants are exposed to elevated temperatures. Moreover, oxidation, which can lead to the formation of sludge and deposits, is a significant factor in the degradation of lubricants. Saturated hydrocarbons are generally more stable against oxidation than unsaturated ones.

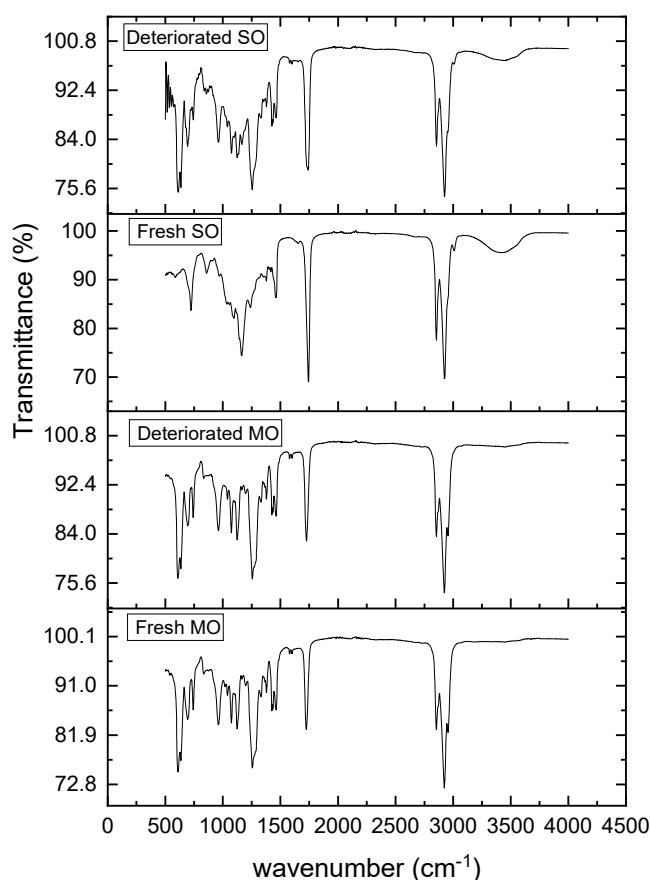


Figure 6. Comparison of FTIR of the CuO-based synthetic lubricant versus the mineral lubricant (Delo).

Around 1733 cm^{-1} , the carbonyl (C=O) functional group was associated with the identified peak. However, the peak in the case of both the fresh and deteriorated synthetic oil was higher than the mineral oil. It depicted the higher content of the carbonyl group in the synthetic oil. The impact of carbonyl groups in lubricant oil is complex and depends on the specific compounds present, their concentration, and the overall lubricant formulation. While some carbonyl-containing compounds may enhance certain properties, others may contribute to oxidation and degradation.

In the peak region around 1258 cm^{-1} , the aromatic amine (C-N) functional group was identified. Both the fresh and synthetic mineral oil showed a higher content of the amine group, as can be seen from the higher peaks in Figure 6 around the wavelengths of 1200 to 1300 cm^{-1} . Aromatic amines can act as antioxidants in lubricant oils, helping to inhibit the oxidation of the oil. Oxidation is a chemical reaction that can lead to the degradation of the lubricant, resulting in increased viscosity, sludge formation, and the generation of acidic

by-products. Aromatic amines scavenge free radicals and prevent oxidative degradation. Aromatic amines are known for their anti-wear properties. They can form a protective film on metal surfaces, reducing friction and wear between moving parts. This is particularly important in high-load and high-temperature applications. Aromatic amines can contribute to the extreme pressure (EP) characteristics of lubricant operations. In situations where metal surfaces experience extreme pressure, such as in gear applications, aromatic amines can help form a lubricating film that prevents metal-to-metal contact and reduces wear. Aromatic amines can serve as detergents and dispersants in lubricant formulations. They help keep the engine or machinery components clean by preventing the formation of deposits and by dispersing any particles that do form. This contributes to the overall cleanliness and efficiency of the lubrication system.

The last peak was formed around 609 cm^{-1} . It showed the presence of the alkyl halide (C-Br) functional group. The mineral oil possessed higher peaks than the synthetic oil around the 600 cm^{-1} wavelength. Lubricant oils with alkyl halides may pose environmental concerns due to the potential release of halogenated compounds during use or disposal. Halogenated compounds can be persistent and may have adverse effects on the environment. As alkyl halides are generally reactive compounds, they can undergo various chemical reactions, including hydrolysis, which may lead to the formation of acidic by-products. The reactivity of alkyl halides could contribute to undesirable effects on the lubricant's stability.

The distinct regions of the novel and conventional lubricants are depicted in Figure 6. The narrow peak in the first portion has a range of approximately $3187\text{--}3628\text{ cm}^{-1}$. The results of the range of the first peak indicate that the O-H functional group is associated with the IR chart. The second narrow stretch peak depicts the presence of a functional group of alkanes (C-H). The third peak is in the single-bonded portion that also contains the alkane group with a value of 2926 cm^{-1} . The latter two peaks also lie in the range of the alkane functional group with the values of 2882 cm^{-1} and 2856 cm^{-1} . The C=O functional group is associated with the peak around 1733 cm^{-1} . The C-N functional group is in the fourth fingerprint portion, where the value of the peak is 1258 cm^{-1} . The C-Br functional group is associated with the bottommost peak at 609 cm^{-1} . The shifting in the peaks was observed because of contamination and a high temperature in the engine.

3.3. Atomic Absorption Spectroscopy (AAS)

The AAS technique is utilized to classify distinct metals in selected lubricant oil samples [67]. To calculate the number of various metals in the desired samples of a lubricant, an AAS apparatus was utilized, which operated on the flame with the desired wavelength of the bulb. The machine was equipped with the same type of bulb to determine a specific atom or element. AAS works on the principle that atoms or ions with a specific wavelength absorb light. The atom absorbs the energy (light), and a particular wavelength of light is produced [68,69]. To determine the number of desired atoms or ions in the novel and conventional lubricants before and after use, salt solutions of the desired atoms or ions were first prepared. In this way, unique samples of the desired metal were produced with the unique salt at the needed ppm. The mean absorbance of the required metal in the conventional and novel lubricants was then determined utilizing an AAS machine based on the standards. The mechanical assemblies in automobiles majorly constitute iron-based alloys. Therefore, the worn bearings, crankshafts, piston rings, cylinder valves, etc., are primarily accountable for iron (Fe) existence in lubricant oil. The journal and piston jacket are usually manufactured from aluminum (Al) due to its lower density and higher heat transfer rate [70]. Therefore, aluminum particles indicate wear in the journal and piston jackets. Copper alloys are used to manufacture intermediate layers of engine bearings, and the presence of copper inside lubricant oil depicts wear in such layers. The piston rings, crankshaft, and cylinder liners are mainly composed of chromium, and they serve as potential sources of chromium in lubricant oil as a result of their wearing [71]. A spectrophotometer designed by Spectroil was used to identify wear debris in compliance

with the ASTM D-6595 standard [72]. Additive depletion analysis was used to evaluate the proportion of performance additives in the lubricant oil. Zinc, being an anti-wear particle in lubricant oils, provides a lower friction coating in order to protect a metal. However, calcium is a detergent additive used to neutralize the combustion byproducts because of its acidic character [73]. Table 7 shows the atomic absorption spectroscopy results for pre- and post-operations of the mineral and synthetic oils.

Table 7. AAS for sample lubricants.

AAS of Distinct Elements				
Sr.	Element Types	Lubricant Types	Mean Absorbance	
			Pre-Operation	Post-Operation
1	Chromium (Cr)	Mineral	3.32	3.45
		Novel	4.46	5.60
2	Iron (Fe)	Mineral	2.13	2.10
		Novel	2.20	2.24
3	Copper (Cu)	Mineral	3.49	4.29
		Novel	4.39	4.75
4	Zinc (Zn)	Mineral	5.61	3.81
		Novel	3.1	2.77
5	Aluminium (Al)	Mineral	2.39	2.41
		Novel	2.42	2.47
6	Calcium (Ca)	Mineral	2.48	2.37
		Novel	6.51	5.07

3.3.1. Chromium (Cr) AAS

Figure 7 demonstrates that after 100 h of C.I. engine operations, the proportion of chromium (Cr) metal in the novel lubricant raised from 4.46 to 5.6 ppm. In the same way, the amount of Cr metal in the Delo-based conventional lubricant increased from 3.32 to 3.45 ppm after 100 h of C.I. engine operations. Thus, it is evident that when running the engine, wear and the coefficient of friction caused the Cr concentration to increase.

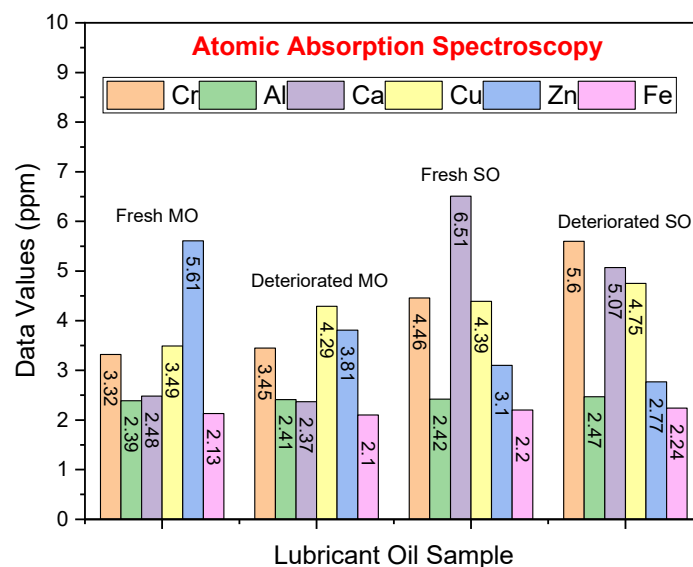


Figure 7. AAS of lubricant oil samples.

3.3.2. Aluminum (Al) AAS

Figure 7 shows that after 100 h of C.I. engine operations, the proportion of aluminum metal in the novel lubricant rose from 2.42 to 2.47 ppm. In the same way, the amount of Al metal in the Delo-based conventional lubricant increased from 2.39 to 2.41 ppm, subsequent to 100 h of C.I. engine operations. Thus, it is evident that when running the engine, wear and the coefficient of friction caused the Al concentration to increase.

3.3.3. Calcium (Ca) AAS

Figure 7 shows that after 100 h of C.I. engine operations, the proportion of Ca metal in the novel lubricant declined from 6.51 to 5.07 ppm. Similarly, the amount of calcium metal in the Delo-based conventional lubricant also decreased from 2.48 to 2.37 ppm. The percentage decrease in the fresh and used novel lubricants was 22.11%, while in the Delo-based conventional lubricant, the percentage decrease was merely 4.43%.

3.3.4. Copper (Cu) AAS

Figure 7 shows that after 100 h of C.I. engine operations, the proportion of Cu metal in the novel lubricant increased from 4.39 to 4.75 ppm. Similarly, the amount of copper metal in the Delo-based conventional lubricant also increased from 3.49 to 4.29 ppm after using the C.I. engine for 100 h. Thus, it is evident that while running the engine, wear and the coefficient of friction caused the Cu concentration to increase. The increase in Cu concentration after using the novel lubricant was 8.2%, while for the Delo-based conventional lubricant, it was 22.29%. So, 14.09% more wear-and-tear of copper was observed in the Delo-based conventional lubricant as compared with the novel lubricant.

3.3.5. Zinc (Zn) AAS

Figure 7 shows that after 100 h of C.I. engine operations, the proportion of Zn metal in the novel lubricant declined from 3.1 to 2.77 ppm. Similarly, the amount of Zn metal in the Delo-based conventional lubricant also decreased from 5.61 ppm to 3.81 ppm after using the C.I. engine for 100 h.

3.3.6. Iron (Fe) AAS

Figure 7 shows that after 100 h of C.I. engine operations, the proportion of iron metal in the novel lubricant increased from 2.20 to 2.25 ppm. Similarly, the amount of iron metal in the Delo-based conventional lubricant also increased from 2.13 to 2.16 ppm after using the C.I. engine for 100 h. Thus, it is evident that while running the engine, wear and the coefficient of friction caused the Fe concentration to increase. An increase of 2.72% in the Fe concentration was observed after using the novel lubricant, while in the Delo-based conventional lubricant, it was 1.76%. Around 35.29% more wear-and-tear of iron was observed in the novel lubricant as compared with the Delo-based lubricant.

4. Conclusions

The physicochemical analysis reveals that the specific gravity and flash point of the CuO-based novel lubricant are nearly equivalent to those of the conventional lubricant with deteriorations of 0.29% and 1.6%, respectively. However, the novel lubricant proved to be better than the conventional oil in terms of ash content and $(KV)_{40\text{ }^{\circ}\text{C}}$, with improvements of 4.18% and 1.15%, respectively. However, in the case of the PP, TBN, and $(KV)_{100\text{ }^{\circ}\text{C}}$, the deterioration rate of the novel lubricant was better than the mineral lubricant with values of 1.27%, 6.37%, and 1.43%, respectively.

All peaks of the novel and mineral lubricants overlapped with each other and contained functional groups including C=O, C-H, C-N, O-H, and C-Br, as can be seen from three sections of the mid-infrared spectra from 4000 to 1500 cm^{-1} . However, synthetic lubricants possess higher transmittance than mineral oils and enable better monitoring, early detection of potential issues, and improved functionality in various applications.

The AAS testing shows that the synthetic oil possesses 21.64%, 3.23%, 21.44%, and 1.23% higher chromium, iron, aluminum, and zinc content. However, the copper and calcium contents in the synthetic oil are 14.72 and 17.68%, respectively.

It is concluded that because of its optimum viscosities, higher densities, lower reductions in friction, and most importantly, eco-friendly nature, the CuO-based novel lubricant can be utilized as an alternative to mineral lubricants. In the future, researchers can use alternative nanoparticles to further improve lubricant oil characteristics to achieve better outcomes. The direct impact of these bio-lubricants on engine exhaust emissions and engine performance needs to be investigated in order to comply with the sustainable development goals of the United Nations Vision 2030.

Author Contributions: Writing—original draft and investigation, A.S.N.; conceptualization, resources, M.U.; project administration, M.A.I.M.; methodology and data curation, A.N.S.; writing—review and editing, A.T.J., M.W.S., U.S. and N.A.; supervision, validation, N.A.; formal analysis, M.R.K. and M.A.K. All authors have read and agreed to the published version of the manuscript.

Funding: The authors extend their appreciation to the Researchers Supporting Project number (RSPD2023R956), King Saud University, Riyadh, Saudi Arabia.

Institutional Review Board Statement: Not applicable.

Informed Consent Statement: Not applicable.

Data Availability Statement: No new data were created or analyzed in this study. Data sharing is not applicable to this article.

Conflicts of Interest: The authors declare no conflict of interest.

References

- Sanchez, C.J. *Tribological Characterization of Carbon Based Solid Lubricants*; Texas A & M University: College Station, TX, USA, 2012.
- Woldegebriel Gebretsadik, D.; Hardell, J.; Efeoglu, I.; Prakash, B. Tribological Properties of Composite Multilayer Coatings. *Tribol. Mater. Surf. Interfaces* **2011**, *5*, 100–106. [[CrossRef](#)]
- Holmberg, K.; Andersson, P.; Erdemir, A. Global energy consumption due to friction in passenger cars. *Tribol. Int.* **2012**, *47*, 221–234. [[CrossRef](#)]
- Will, F. Fuel conservation and emission reduction through novel waste heat recovery for internal combustion engines. *Fuel* **2012**, *102*, 247–255. [[CrossRef](#)]
- Pinkus, O.; Wilcock, D.F. *Strategy for Energy Conservation through Tribology*; American Society of Mechanical Engineers: New York, NY, USA, 1977.
- Dake, L.; Russell, J.; Debrodt, D. A review of DOE ECUT tribology surveys. *J. Tribol.* **1986**, *108*, 497–501. [[CrossRef](#)]
- Ouyang, P.; Zhang, X. Regeneration of the waste lubricating oil based upon flyash adsorption/solvent extraction. *Environ. Sci. Pollut. Res.* **2020**, *27*, 37210–37217. [[CrossRef](#)] [[PubMed](#)]
- Mujtaba, M.; Masjuki, H.; Kalam, M.; Noor, F.; Farooq, M.; Ong, H.C.; Gul, M.; Soudagar, M.E.M.; Bashir, S.; Rizwanul Fattah, I. Effect of additivized biodiesel blends on diesel engine performance, emission, tribological characteristics, and lubricant tribology. *Energies* **2020**, *13*, 3375. [[CrossRef](#)]
- Singh, A.; Chauhan, P.; Mamatha, T. A review on tribological performance of lubricants with nanoparticles additives. *Mater. Today Proc.* **2020**, *25*, 586–591. [[CrossRef](#)]
- Vafadar, A.; Guzzomi, F.; Rassau, A.; Hayward, K. Advances in metal additive manufacturing: A review of common processes, industrial applications, and current challenges. *Appl. Sci.* **2021**, *11*, 1213. [[CrossRef](#)]
- Tung, S.C.; Totten, G.E. *Automotive Lubricants and Testing*; ASTM International: West Conshohocken, PA, USA, 2012.
- Stachowiak, G.W.; Batchelor, A.W. *Engineering Tribology*; Butterworth-Heinemann: Oxford, UK, 2013.
- Rashid, M.I.; Yaqoob, Z.; Mujtaba, M.; Fayaz, H.; Saleel, C.A. Developments in mineral carbonation for Carbon sequestration. *Heliyon* **2023**, *9*, e21796. [[CrossRef](#)]
- Tung, S.; Totten, G. Gear Oil Screen Testing with FZG Back-to-Back Rig. In *Automotive Lubricants and Testing*; ASTM International: West Conshohocken, PA, USA, 2012.
- Shafi, W.K.; Raina, A.; Ul Haq, M.I. Friction and wear characteristics of vegetable oils using nanoparticles for sustainable lubrication. *Tribol. Mater. Surf. Interfaces* **2018**, *12*, 27–43. [[CrossRef](#)]
- Jeevan, T.; Jayaram, S.; Afzal, A.; Ashrith, H.; Soudagar, M.E.M.; Mujtaba, M. Machinability of AA6061 aluminum alloy and AISI 304L stainless steel using nonedible vegetable oils applied as minimum quantity lubrication. *J. Braz. Soc. Mech. Sci. Eng.* **2021**, *43*, 159. [[CrossRef](#)]
- Hamrock, B.J.; Schmid, S.R.; Jacobson, B.O. *Fundamentals of Fluid Film Lubrication*; CRC Press: Boca Raton, FL, USA, 2004.

18. McNutt, J. Development of biolubricants from vegetable oils via chemical modification. *J. Ind. Eng. Chem.* **2016**, *36*, 1–12. [[CrossRef](#)]
19. Noori, A.A.S.; Hussein, H.A.; Namer, N.S. Influence of adding CuO and MoS₂ nano-particles to castor oil and moulding oil on tribological properties. *Proc. IOP Conf. Ser. Mater. Sci. Eng.* **2019**, *518*, 032040. [[CrossRef](#)]
20. Salimon, J.; Salih, N.; Yousif, E. Industrial development and applications of plant oils and their biobased oleochemicals. *Arab. J. Chem.* **2012**, *5*, 135–145. [[CrossRef](#)]
21. Syahir, A.; Zulkifli, N.; Masjuki, H.; Kalam, M.; Alabdulkarem, A.; Gulzar, M.; Khuong, L.; Harith, M.H. A review on bio-based lubricants and their applications. *J. Clean. Prod.* **2017**, *168*, 997–1016. [[CrossRef](#)]
22. Singh, A.K. Castor oil-based lubricant reduces smoke emission in two-stroke engines. *Ind. Crops Prod.* **2011**, *33*, 287–295. [[CrossRef](#)]
23. Bongfa, B.; Peter, A.A.; Barnabas, A.; Adeotic, M.O. Comparison of lubricant properties of castor oil and commercial engine oil. *J. Tribol.* **2015**, *5*, 1–11.
24. Gulzar, M.; Masjuki, H.; Varman, M.; Kalam, M.; Mufti, R.; Zulkifli, N.; Yunus, R.; Zahid, R. Improving the AW/EP ability of chemically modified palm oil by adding CuO and MoS₂ nanoparticles. *Tribol. Int.* **2015**, *88*, 271–279. [[CrossRef](#)]
25. Akhtar, N.; Adnan, Q.; Ahmad, M.; Mehmood, A.; Farzana, K. Rheological studies and characterization of different oils. *J. Chem. Soc. Pak.* **2009**, *31*, 201–206.
26. Imran, S.; Gul, M.; Kalam, M.; Zulkifli, N.; Mujtaba, M.; Yusoff, M.; Awang, M. Effect of various nanoparticle biodiesel blends on thermal efficiency and exhaust pollutants. *Int. J. Energy Environ. Eng.* **2023**, *14*, 937–948. [[CrossRef](#)]
27. Abdel-Rehim, A.A.; Akl, S.; Elsouady, S. Investigation of the tribological behavior of mineral lubricant using copper oxide nano additives. *Lubricants* **2021**, *9*, 16. [[CrossRef](#)]
28. Namer, N.S.; Nama, S.A.; Mezher, M.T. The influence of nano particles additive on tribological properties of aa2024-t4 coated with tin or sin thin films. *J. Mech. Eng. Res. Dev.* **2019**, *42*, 30–34. [[CrossRef](#)]
29. Raina, A.; Anand, A. Tribological investigation of diamond nanoparticles for steel/steel contacts in boundary lubrication regime. *Appl. Nanosci.* **2017**, *7*, 371–388. [[CrossRef](#)]
30. Najan, A.; Navthar, R.; Gitay, M. Experimental Investigation of tribological properties using nanoparticles as modifiers in lubricating oil. *Int. Res. J. Eng. Technol.* **2017**, *4*, 1125–1129.
31. Popoola, C.A.; Ogundola, J.; Kamtu, P. Tribological properties of copper (II) oxide nanoparticle-enriched sandbox bio-lubricant. *Glob. J. Eng. Technol. Adv.* **2021**, *8*, 8–19. [[CrossRef](#)]
32. Baskar, S.; Sriram, G.; Arumugam, S. Tribological analysis of a hydrodynamic journal bearing under the influence of synthetic and biolubricants. *Tribol. Trans.* **2017**, *60*, 428–436. [[CrossRef](#)]
33. Sukkar, K.A.; Karamalluh, A.A.; Jaber, T.N. Rheological and thermal properties of lubricating oil enhanced by the effect of CuO and TiO₂ nano-additives. *Al-Khwarizmi Eng. J.* **2019**, *15*, 24–33. [[CrossRef](#)]
34. Fayad, M.A.; AL-Ogaidi, B.R.; Abood, M.K.; AL-Salihi, H.A. Influence of post-injection strategies and CeO₂ nanoparticles additives in the C30D blends and diesel on engine performance, NOX emissions, and PM characteristics in diesel engine. *Part. Sci. Technol.* **2022**, *40*, 824–837. [[CrossRef](#)]
35. Esfe, M.H.; Kamyab, M.H.; Ardeshiri, E.M.; Toghraie, D. Study of MWCNT (40%)–CuO (60%)/10W40 hybrid nanofluid for improving laboratory oil performance by laboratory method and statistical response surface methodology. *Alex. Eng. J.* **2023**, *63*, 115–125. [[CrossRef](#)]
36. Al-Tabbakh, B.A.A.; Jaed, D.M.; Qubian, N.A.; Kareem, S. Preparation of CuO Nanoparticles for Improving Base Oil Properties. *J. Pet. Res. Stud.* **2022**, *12*, 191–205.
37. Navada, M.K.; Rai, R.; Ganesha, A.; Patil, S. Synthesis and characterization of size controlled nano copper oxide structures for antioxidant study and as eco-friendly lubricant additive for bio-oils. *Ceram. Int.* **2023**, *49*, 10402–10410. [[CrossRef](#)]
38. Kumar, D.S.; Garg, H.; Kumar, G. Tribological analysis of blended vegetable oils containing CuO nanoparticles as an additive. *Mater. Today Proc.* **2022**, *51*, 1259–1265. [[CrossRef](#)]
39. Gupta, H.; Rai, S.K.; Satya Krishna, N.; Anand, G. The effect of copper oxide nanoparticle additives on the rheological and tribological properties of engine oil. *J. Dispers. Sci. Technol.* **2021**, *42*, 622–632. [[CrossRef](#)]
40. Subedi, B.R.; Trital, H.M.; Rajbhandari, A. Characterization of CuO-Nanoadditive Blended Engine Oil. *J. Inst. Sci. Technol.* **2017**, *22*, 152–158. [[CrossRef](#)]
41. Ghaednia, H.; Jackson, R.L.; Khodadadi, J.M. Experimental analysis of stable CuO nanoparticle enhanced lubricants. *J. Exp. Nanosci.* **2015**, *10*, 1–18. [[CrossRef](#)]
42. Shah, A.K.; Vineesh, K.; Joy, M. Study of the lubricating properties of hybrid liquid paraffin with TiO₂ and CuO as nano-additives for engine oil application. *Proc. IOP Conf. Ser. Mater. Sci. Eng.* **2019**, *624*, 012006. [[CrossRef](#)]
43. Hassan, M.U.; Usman, M.; Bashir, R.; Naeem Shah, A.; Ijaz Malik, M.A.; Mujtaba, M.; Elkhateb, S.E.; Kalam, M.A. Tribological Analysis of Molybdenum Disulfide (MOS₂) Additivated in the Castor and Mineral Oil Used in Diesel Engine. *Sustainability* **2022**, *14*, 10485. [[CrossRef](#)]
44. Hosseinzadeh-Bandbafha, H.; Tabatabaei, M.; Aghbashlo, M.; Khanali, M.; Demirbas, A. A comprehensive review on the environmental impacts of diesel/biodiesel additives. *Energy Convers. Manag.* **2018**, *174*, 579–614. [[CrossRef](#)]
45. Rastogi, P.; Kumar, N.; Sharma, A.; Vyas, D.; Gajbhiye, A. Sustainability of aluminium oxide nanoparticles blended mahua biodiesel to the direct injection diesel engine performance and emission analysis. *Pollution* **2020**, *6*, 25–33.

46. D'Silva, R.; Vinoothan, K.; Binu, K.; Thirumaleshwara, B.; Raju, K. Effect of titanium dioxide and calcium carbonate nanoadditives on the performance and emission characteristics of CI engine. *J. Mech. Eng. Autom.* **2016**, *6*, 28–31.
47. Mello, V.; Faria, E.; Alves, S.; Scandian, C. Enhancing CuO nanolubricant performance using dispersing agents. *Tribol. Int.* **2020**, *150*, 106338. [[CrossRef](#)]
48. Pisal, A.S.; Chavan, D. Experimental investigation of tribological properties of engine oil with CuO nanoparticles. *Res. Mech. Eng.* **2014**, *2014*, 49.
49. Diegelmann, S.R.; Parks, B.W. TBN and Performance Booster. 2017. Available online: <https://patentimages.storage.googleapis.com/26/f4/f2/b17895edad4930/US20170292083A1.pdf> (accessed on 15 September 2023).
50. Huang, Y.; Li, F.; Bao, G.; Wang, W.; Wang, H. Estimation of kinematic viscosity of biodiesel fuels from fatty acid methyl ester composition and temperature. *J. Chem. Eng. Data* **2020**, *65*, 2476–2485. [[CrossRef](#)]
51. Curtis, M.; Aduse-Opoku, J.; Slaney, J.; Rangarajan, M.; Booth, V.; Cridland, J.; Shepherd, P. Characterization of an adherence and antigenic determinant of the ArgI protease of *Porphyromonas gingivalis* which is present on multiple gene products. *Infect. Immun.* **1996**, *64*, 2532–2539. [[CrossRef](#)] [[PubMed](#)]
52. Stanciu, I. Some Methods for Determining the Viscosity Index of Hydraulic Oil. *Indian J. Sci. Technol.* **2023**, *16*, 254–258. [[CrossRef](#)]
53. Jamil, M.K.; Akhtar, M.; Farooq, M.; Abbas, M.M.; Saad, M.; Khuzaima, M.; Ahmad, K.; Kalam, M.A.; Abdelrahman, A. Analysis of the Impact of Propanol-Gasoline Blends on Lubricant Oil Degradation and Spark-Ignition Engine Characteristics. *Energies* **2022**, *15*, 5757. [[CrossRef](#)]
54. Malik, M.A.I.; Kalam, M.; Mujtaba, M.; Almomani, F. A review of recent advances in the synthesis of environmentally friendly, sustainable, and nontoxic bio-lubricants: Recommendations for the future implementations. *Environ. Technol. Innov.* **2023**, *32*, 103366. [[CrossRef](#)]
55. Kaminski, P. Experimental investigation into the effects of fuel dilution on the change in chemical properties of lubricating oil used in fuel injection pump of pielstick PA4 V185 marine diesel engine. *Lubricants* **2022**, *10*, 162. [[CrossRef](#)]
56. Abdelkhalik, A.; Elsayed, H.; Hassan, M.; Nour, M.; Shehata, A.; Helmy, M. Using thermal analysis techniques for identifying the flash point temperatures of some lubricant and base oils. *Egypt. J. Pet.* **2018**, *27*, 131–136. [[CrossRef](#)]
57. Mujtaba, M.; Kalam, M.; Masjuki, H.; Gul, M.; Soudagar, M.E.M.; Ong, H.C.; Ahmed, W.; Atabani, A.; Razzaq, L.; Yusoff, M. Comparative study of nanoparticles and alcoholic fuel additives-biodiesel-diesel blend for performance and emission improvements. *Fuel* **2020**, *279*, 118434. [[CrossRef](#)]
58. Hettiarachchi, S.J.; Kellici, S.; Kershaw, M.; Bowen, J. Enhancing physicochemical properties of coconut oil for the application of engine lubrication. *Tribol. Int.* **2023**, *190*, 109060. [[CrossRef](#)]
59. Niu, Y.; Pang, X.; Yue, S.; Shangguan, B.; Zhang, Y. The friction and wear behavior of laser textured surfaces in non-conformal contact under starved lubrication. *Wear* **2021**, *476*, 203723. [[CrossRef](#)]
60. Abro, R.; Chen, X.; Harijan, K.; Dhakan, Z.A.; Ammar, M. A Comparative study of recycling of used engine oil using extraction by composite solvent, single solvent, and acid treatment methods. *ISRN Chem. Eng.* **2013**, *2013*, 952589. [[CrossRef](#)]
61. Ijaz Malik, M.A.; Usman, M.; Akhtar, M.; Farooq, M.; Saleem Iqbal, H.M.; Irshad, M.; Shah, M.H. Response surface methodology application on lubricant oil degradation, performance, and emissions in SI engine: A novel optimization of alcoholic fuel blends. *Sci. Prog.* **2023**, *106*, 00368504221148342. [[CrossRef](#)] [[PubMed](#)]
62. Wolak, A.; Molenda, J.; Zając, G.; Janocha, P. Identifying and modelling changes in chemical properties of engine oils by use of infrared spectroscopy. *Measurement* **2021**, *186*, 110141. [[CrossRef](#)]
63. Patel, N.; Shadangi, K.P.; Kar, P.K. Characterization of waste engine oil derived pyrolytic char (WEOPC): SEM, EDX and FTIR analysis. *Mater. Today Proc.* **2021**, *38*, 2866–2870. [[CrossRef](#)]
64. Abdul-Munaim, A.M.; Holland, T.; Sivakumar, P.; Watson, D.G. Absorption wavebands for discriminating oxidation time of engine oil as detected by FT-IR spectroscopy. *Lubricants* **2019**, *7*, 24. [[CrossRef](#)]
65. Liu, Y.; Bao, K.; Wang, Q.; Zio, E. Application of FTIR method to monitor the service condition of used diesel engine lubricant oil. In Proceedings of the 2019 4th International Conference on System Reliability and Safety (ICSRS), Rome, Italy, 20–22 November 2019; pp. 175–180.
66. van de Voort, F.R. FTIR Condition Monitoring of In-Service Lubricants: Analytical Role and Quantitative Evolution. *Tribol. Online* **2022**, *17*, 144–161. [[CrossRef](#)]
67. Dos Santos, H.S.; De Jesus, A.; Laroque, D.O.; Piatnicki, C.M.; Da Silva, M.M. Multi-element determination of trace elements in B7-diesel Oil by high-resolution continuum source flame atomic absorption spectrometry. *Braz. J. Anal. Chem.* **2021**, *8*, 59–70. [[CrossRef](#)]
68. Kurre, S.; Pandey, S.; Khatri, N.; Bhurat, S.; Kumawat, S.; Saxena, S.; Kumar, S. Study of lubricating oil degradation of CI engine fueled with diesel-ethanol blend. *Tribol. Ind.* **2021**, *43*, 222. [[CrossRef](#)]
69. Manjusha, R.; Shekhar, R.; Kumar, S.J. Ultrasound-assisted extraction of Pb, Cd, Cr, Mn, Fe, Cu, Zn from edible oils with tetramethylammonium hydroxide and EDTA followed by determination using graphite furnace atomic absorption spectrometer. *Food Chem.* **2019**, *294*, 384–389. [[CrossRef](#)] [[PubMed](#)]
70. Widowati, A.; Wakid, M. Study of piston from the natural science perspective. *AIP Conf. Proc.* **2023**, *2671*, 020013.
71. Usman, M.; Khan, T.; Riaz, F.; Ijaz Malik, M.A.; Amjad, M.T.; Shah, M.H.; Ashraf, W.M.; Krzywanski, J.; Nowak, W. Acetone-Gasoline Blend as an Alternative Fuel in SI Engines: A Novel Comparison of Performance, Emission, and Lube Oil Degradation. *ACS Omega* **2023**, *8*, 11267–11280. [[CrossRef](#)] [[PubMed](#)]

72. Malinowska, M. Spectroscopic study and analysis of the content of residue elements in Marinol RG 1240 oil after working in various types of engines. *Zesz. Nauk. Akad. Morskiej Gdyni* **2017**, 131–140.
73. Usman, M.; Malik, M.A.I.; Ranjha, Q.A.; Arif, W.; Jamil, M.K.; Miran, S.; Siddiqui, S. Experimental assessment of performance, emission and lube oil deterioration using gasoline and LPG for a sustainable environment. *Case Stud. Therm. Eng.* **2023**, *49*, 103300. [[CrossRef](#)]

Disclaimer/Publisher's Note: The statements, opinions and data contained in all publications are solely those of the individual author(s) and contributor(s) and not of MDPI and/or the editor(s). MDPI and/or the editor(s) disclaim responsibility for any injury to people or property resulting from any ideas, methods, instructions or products referred to in the content.